Turkish Journal of Electrical Engineering & Computer Sciences

http://journals.tubitak.gov.tr/elektrik/

Research Article

Turk J Elec Eng & Comp Sci
(2021) 29: 1692 – 1705
© TÜBİTAK
doi:10.3906/elk-2005-86

# New hyperchaotic system with single nonlinearity, its electronic circuit and encryption design based on current conveyor

**Anitha KARTHIKEYAN**[1], **Serdar ÇİÇEK**[2,*], **Karthikeyan RAJAGOPAL**[3], **Prakash DURAISAMY**[3], **Ashokkumar SRINIVASAN**[3]

[1]Nonlinear Systems and Applications, Faculty of Electrical and Electronics Engineering, Ton Duc Thang University, Ho Chi Minh City, Vietnam
[2]Department of Electronic and Automation, Vocational School of Hacıbektaş, Nevşehir Hacı Bektaş Veli University, Nevşehir, Turkey
[3]Center for Nonlinear Systems, Chennai Institute of Technology, Chennai, India

**Received:** 14.05.2020 • **Accepted/Published Online:** 15.12.2020 • **Final Version:** 31.05.2021

**Abstract:** Nowadays, hyperchaotic system (HCSs) have been started to be used in engineering applications because they have complex dynamics, randomness, and high sensitivity. For this purpose, HCSs with different features have been introduced in the literature. In this work, a new HCS with a single discontinuous nonlinearity is introduced and analyzed. The proposed system has one saddle focus equilibrium. When the dynamic properties and bifurcation graphics of the system are analyzed, it is determined that the proposed system exhibits the complex phenomenon of multistability. Moreover, analog electronic circuit design of the proposed system is performed with positive second-generation current conveyor. In addition, an encryption circuit is designed to demonstrate that the proposed system can be used in various engineering applications.

**Key words:** Hyperchaos, single nonlinearity, multistability, second-generation current conveyor, encryption, electronic circuit design

## 1. Introduction

Hyperchaos has gained importance in communication technologies because of its complex dynamics, randomness, and high sensitivity since from the first known hyperchaotic system was proposed by Rossler [1–3]. Having at least 4 dimensions and at least two unstable directions are important features of hyperchaotic systems (HCS). The randomness and unpredictable nature of HCS are more compared to the general chaotic systems (CSs). Thus, HCSs are useful for engineering applications such as chaos-based cryptography [4, 5] and image encryption [6, 7]. Recently, many new HCSs with various features have been proposed in the literature [8, 9]. These HCSs are as follows: systems without equilibrium points [10, 11], systems with parameter controlled equilibrium points (chameleon) [12], systems with fractional order terms [13], and systems with higher orders [14]. From the literature review given in Table 1, we can clearly see the challenges in HCSs during implementation and the number of nonlinear terms affects the performance of the circuit.

In the literature, conventional operational amplifier (OPAMP) devices have been usually used in analog electronic designs for chaotic systems [15–23]. An OPAMP is a voltage-mode electronic device. The gain-bandwidth product of the OPAMP devices is fixed. Therefore, OPAMP devices have limitations for gain or

*Correspondence: serdarcicek@gmail.com

**Table 1**. Comparison of the proposed hyperchaotic system with other hyperchaotic systems in the literature.

| References | System description | Special properties | Circuit implementation |
|---|---|---|---|
| Barbouza et al., 2008, [40] | 4D hyperchaotic system with 4 nonlinear terms | There are no special properties identified | Circuit implementation done through OPAMP |
| Wei et al., 2017, [41] | 5D Hyperchaotic system with 5 nonlinear terms | Coexistence of attractors | Real-time circuit implementation done through OPAMP |
| Jia 2007, [42] | Hyperchaotic system with 4 nonlinear terms | No special properties discussed | There is no circuit implementation |
| Feng et al., 2015, [43] | Hyperchaotic system with 4 nonlinear terms | No special properties discussed | Circuit implementation done through OPAMP |
| Zheng et al., 2010, [44] | Hyperchaotic system with 4 nonlinear terms | No special properties | There is no circuit implementation |
| Wen-Bo et al., 2011, [45] | Hyperchaotic system with 4 nonlinear terms | Multiscroll property identified | Real-time circuit implementation done through OPAMP |
| Yu et al., 2007, [46] | Hyperchaotic system with 4 nonlinear terms | Multiscroll property identified | Circuit implementation is done through the DSP method. |
| Chen et al., 2011, [47] | Hyperchaotic system with single nonlinear term | No special properties identified | Circuit implantation is not done |
| Zhou et al., 2011, [48] | Hyperchaotic system with single nonlinear term | No special properties identified | Circuit implementation is done through EWB. |
| Yu et al., 2020, [49] | 6D hyperchaotic system with 5 nonlinear terms | Multiple coexisting attractors identified | Circuit implementation is done through FPGA |
| Singh and Roy, 2015, [50] | 4D hyperchaotic system with 3 nonlinear terms | No special properties identified | Real-time circuit implementation done through OPAMP |
| Yu et al., 2020, [51] | Modified Chua's chaotic circuit | Multistability property identified | Circuit implementation through CCII+ |
| This study | 4D hyperchaotic system with single nonlinear term | Multistability property identified. | Circuit implementation done through CCII+ |

operating frequency. Moreover, OPAMPs' slew-rate value is low, dynamic operating range is limited, and power consumption is high [24]. In contrast to these disadvantages of OPAMPs, current-conveyor active devices have the following advantages: bandwidth independent of gain, better frequency performance, higher slew-rate value, better dynamic characteristics, lower power consumption and better integration with integrated circuit technology [24–28]. Due to these advantages of current-conveyor active devices such as operational transconductance amplifiers, current feedback operational amplifiers, unity-gain cells, second-generation current conveyors (CCII) have started to be used in electronic circuit designs for CS [26–30]. In this study, electronic circuit schematic of the proposed new HCS with single nonlinearity is designed based on the positive CCII (CCII+) active devices due to the specified advantages for use in various engineering designs.

As a result of the above discussions, we proposed a new HCS with one nonlinear term. There are only two studies in the literature about single nonlinearity-based hyperchaotic system [31, 32]. However, coexisting attractors and multistability in a single nonlinearity-based hyperchaotic system have not been discussed earlier. Hence, we propose a hyperchaotic system with single nonlinearity and multistability. In addition, an analog design is performed with CCII+ to indicate that the introduced HCS can be used in various engineering applications. The advantage of the proposed HCS is simplicity in structure as well as holding complex special properties, and more importantly, easy & effective implementation.

In Section 2, we introduce and analyze a novel hyperchaotic system (NHS) with single nonlinearity. In Section 3, we present electronic circuit design and results based on positive second-generation current conveyor device of the novel hyperchaotic system with single nonlinearity for use in real engineering applications. In Section 4, we design an encryption application to demonstrate the use of the proposed NHS in practical engineering applications. Lastly, our conclusions are given in Section 5.

## 2. A novel hyperchaotic system (NHS) with single nonlinear term

We introduced a new HCS with a single nonlinearity (1) which is a *signum* discontinuous function. There are no such systems in the literature which can show hyperchaos. The proposed novel HCS is simple according to the number of linear or nonlinear terms as compared with the other similar type of HCS highlighted in Table 1. Hence, it meets one of the criteria for notifying a new chaotic system as described in [33].

$$\begin{aligned} \dot{x} &= a_1 x + a_2 y \\ \dot{y} &= a_3 x + a_4 yzsgn(z) \\ \dot{z} &= a_5 y + a_6 z + a_7 w \\ \dot{w} &= a_8 z + a_9 w + a_{10} x \end{aligned} \tag{1}$$

where $x - y - z - w$ are state variables and from $a_1$ to $a_{10}$ are parameters of the system (1)

The only equilibrium point of the system (1) is the origin $O$. In order to facilitate linearization easier, the nondifferentiable $sgn$ function is replaced by differentiable $hyperbolictan$ function for a smooth approximation. The signum function can be replaced by continuous equivalents $sgn(z) \approx tanh(nz)$, where $n$ is a large constant (refer to Figure 1). We found that when $n$ is small, the hyperbolic tangent is far from the signum function and when $n$ is a large number, the hyperbolic tangent is nearly equal to the signum function and plotted the same in Figure 1. Thus, we choose $n = 100$ for further analysis.

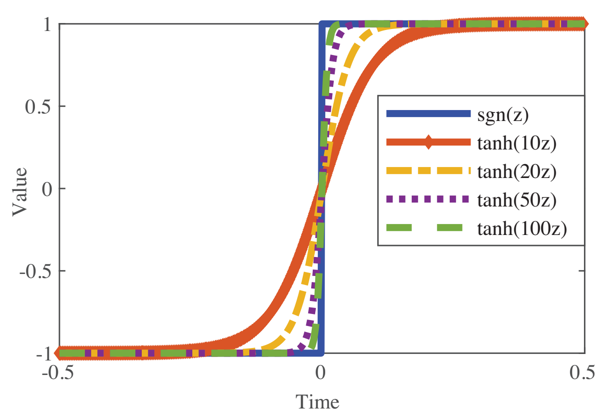


**Figure 1**. The comparison graph showing that the signum function and the hyperbolic tangent function can be used interchangeably.

For this reason, $tanh(100z)$ expression is taken instead of $sgn(z)$ expression. The matrix of Jacobian at equilibrium $O$ is

$$J_0 = \begin{bmatrix} a_1 & a_2 & 0 & 0 \\ a_3 & 0 & 0 & 0 \\ 0 & a_5 & a_6 & a_7 \\ a_{10} & 0 & a_8 & a_9 \end{bmatrix} \tag{2}$$

The characteristic polynomial of the NHS is

$$\lambda^4-(a_1+a_6+a_9)\lambda^3+(a_1a_6-a_2a_3+a_1a_9+a_6a_9-a_7a_8)\lambda^2+)a_2a_3a_6+a_2a_3a_9-a_1a_6a_9+a_1a_7a_8)\lambda-a_2a_3a_6a_9+a_2a_3a_7a_8 \tag{3}$$

If the Routh–Hurwitz criterion is examined as the stability criterion, all minors have to be positive to be stable. Here $\delta_i$ for $i \in [0,4]$ are the coefficients of the characteristic equation with $\delta_0$ being the coefficient of $\lambda^4$. From (3)

$$\begin{aligned}
&\delta_0 = 1;\\
&\delta_1 = -(a_1 + a_6 + a_9)\\
&\delta_2 = (a_1a_6 - a_2a_3 + a_1a_9 + a_6a_9 - a_7a_8)\\
&\delta_3 = (a_2a_3a_6 + a_2a_3a_9 - a_1a_6a_9 + a_1a_7a_8)\\
&\delta_4 = -a_2a_3a_6a_9 + a_2a_3a_7a_8
\end{aligned} \tag{4}$$

The minors are,

$$\Delta_1 = \delta_1 > 0, \quad \Delta_2 = \begin{vmatrix} \delta_1 & \delta_0 \\ \delta_3 & \delta_2 \end{vmatrix} > 0, \Delta_3 = \begin{vmatrix} \delta_1 & \delta_0 & 0 \\ \delta_3 & \delta_2 & \delta_1 \\ 0 & \delta_4 & \delta_3 \end{vmatrix} > 0, \quad \Delta_4 = \begin{vmatrix} \delta_1 & \delta_0 & 0 & 0 \\ \delta_3 & \delta_2 & \delta_1 & \delta_0 \\ 0 & \delta_4 & \delta_3 & \delta_2 \\ 0 & 0 & 0 & \delta_4 \end{vmatrix} > 0 \tag{5}$$

Various combinations of parameters were tried using computer search algorithm (forward continuation method) and the system's parameters values were found in this way. In this way, the values of the obtained parameters for the system are given in Eq. (6).

$$\begin{aligned}
a_1 = 0.75; a_2 = -1.2; a_3 = 1; a_4 = -0.1; a_5 = -1;\\
a_6 = -1.2; a_7 = -5; a_8 = 1; a_9 = 0.8; a_{10} = -0.1
\end{aligned} \tag{6}$$

The dimension of Kaplan–Yorke of the NHS (1) was obtained as $D_{KY} = 3.2$. The eigen values of the NHS for parameter values as in (5) are $\lambda_{1,2} = 0.35 \pm 1.038i$, $\lambda_{3,4} = -0.2 \pm 2i$, which indicates that the equilibrium is a saddle focus. Moreover, the principal minors (4) are $\Delta_1 = -0.3$; $\Delta_2 = 0.86$; $\Delta_3 = -2.46$; $\Delta_4 = -11.91$. As the minors are negative, the equilibrium is unstable. The initial values were taken as $(x_0 = 0.1, y_0 = 0.1, z_0 = 0.1, w_0 = 0.1)$. In Figure 2, the phase characterization of the NHS is given for the parameters as given in (6).

The bifurcation-diagrams are derived to investigate the dynamic behavior of the NHS for changes in parameter values. The parameter $a_1$ is considered to be the control variable while the other variable is kept to the related values as in (6). Forward continuation method is used to find the parameter range, we concentrated the parameter value which shows limit cycle and progress to unbounded case. The bifurcation-diagram of NHS is given in Figure 2. Also seen in Figure 2 that the NHS has chaotic oscillations for $0.674 \leq a_1 \leq 0.75$ and is unbounded when $a_1 > 0.75$. Moreover, the NHS shows a wider tori region for $0.42 \leq a_1 \leq 0.674$.

In order to search the multistability nature of the proposed system, we were provided the bifurcation plots using forward continuation. The parameter value is increased with reinitializing the initial values to the end. In

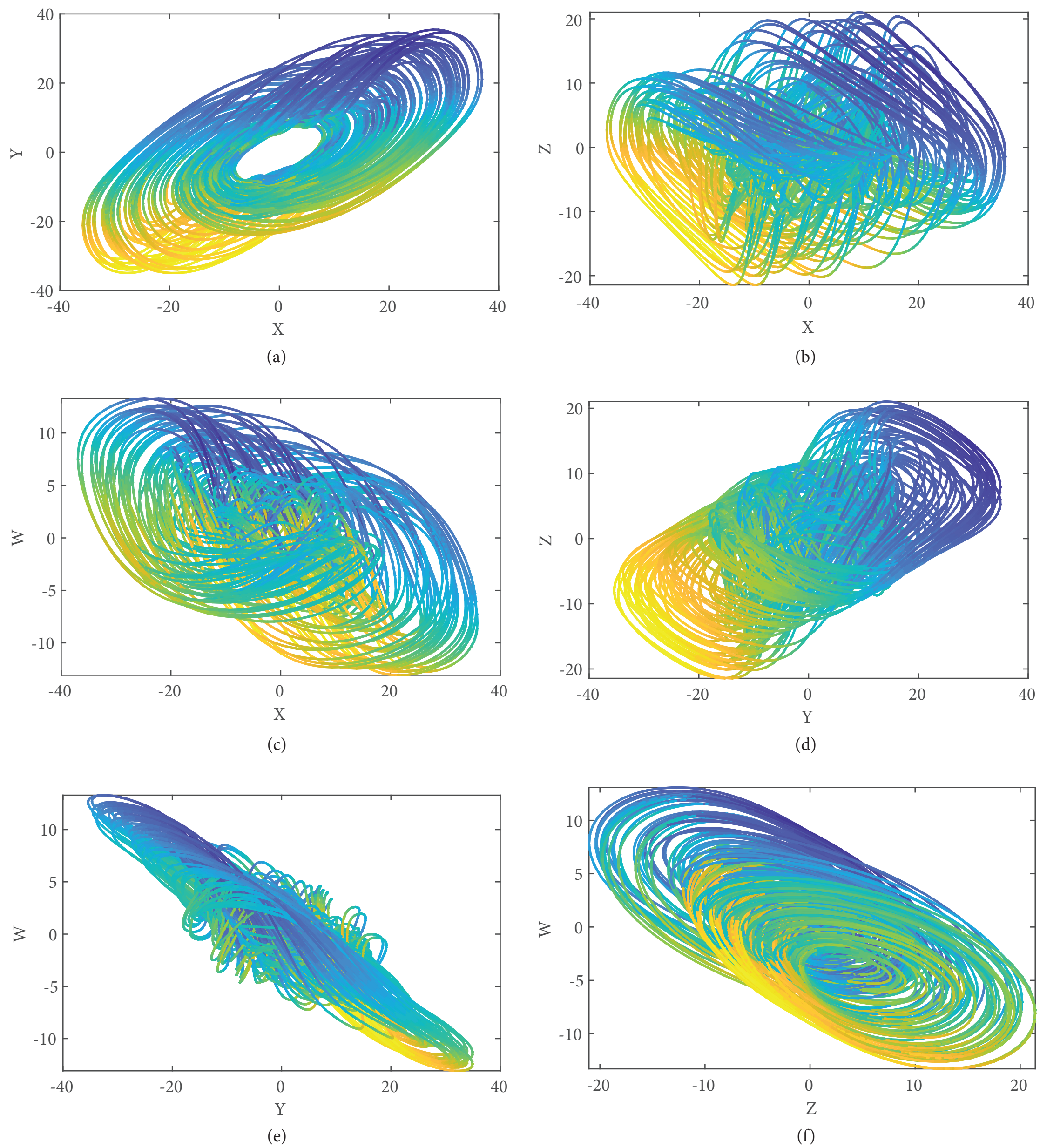


**Figure 2**. Phase characterization of the NHS for the parameters as in (6) with initial values ($x_0 = 0.1, y_0 = 0.1, z_0 = 0.1, w_0 = 0.1$) (a) for $x$-versus-$y$ state variables, (b) for $x$-versus-$z$ state variables, (c) for $x$-versus-$w$ state variables, (d) for $y$-versus-$z$ state variables, (e) for $y$-versus-$w$ state variables, (f) for $z$-versus-$w$ state variables.

addition, backward continuation, which is similar to forward continuation except the parameter, is decreased. Figure 4a shows forward (blue) and backward (red) plots with the respective LEs shown in Figures 4b (forward) and 4c (backward). The NHS shows several coexisting limit cycles and tori between $0.42 \leq a_1 \leq 0.6379$ and shows coexisting limit cycle with hyperchaotic attractor for $0.7138 \leq a_1 \leq 0.7215$. Coexisting hyperchaotic attractors are seen in the range of $0.7216 \leq a_1 \leq 0.7328$. Lyapunov exponents (LEs) were computed using the Wolfs algorithm [34]. The LEs were calculated as $L_1 = 0.097$, $L_2 = 0.023$, $L_3 = 0$, and $L_4 = -0.548$. The LEs signs are $(+, +, 0, -)$ and confirm that the system has hyperchaotic behavior.

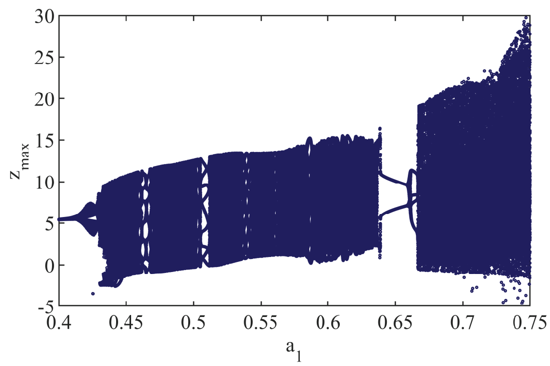


**Figure 3**. Bifurcation diagram of NHS with parameter $a_1$ to observe chaotic regions with the initial condition $(x_0 = 0.1, y_0 = 0.1, z_0 = 0.1, w_0 = 0.1)$.

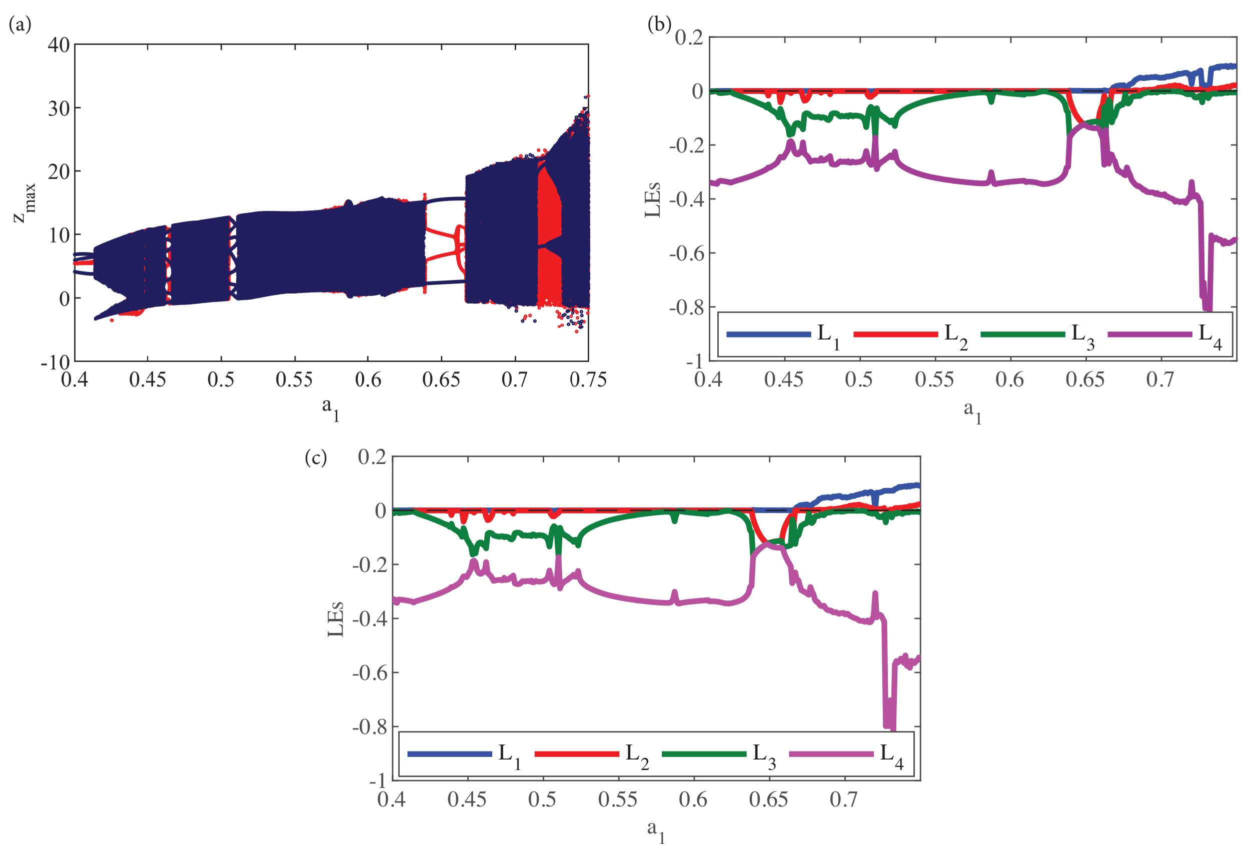


**Figure 4**. Bifurcation diagram and Lyapunov exponents graphs of NHS to observe chaotic regions (a) forward progression (blue) and backward progression (red) for parameter $a_1$, (b) the LEs for forward progression for parameter $a_1$, (c) the LEs for backward progression for parameter $a_1$. The initial values for the first iteration in both forward and backward progression are taken as $(x_0 = 0.1, y_0 = 0.1, z_0 = 0.1, w_0 = 0.1)$.

### 3. Electronic circuit design of the NHS based on CCII± components

The electronic circuit design was realized based on current conveyor of the novel HCS for use in real engineering applications such as cryptography and communication [35–37]. CCII+ is used as a current conveyor in the design. CCII was presented in 1970 by Sedra and Smith in the literature [38]. The general structure of the CCII± is given in Figure 5. The mathematical model of CCII± is as in Eq. (7). In Eq. (7), ± symbol refers to the type of CCII. If the symbol is "+", it denotes positive CCII (CCII+), and if the symbol is "-", it denotes negative CCII ( CCII-) [38, 39].

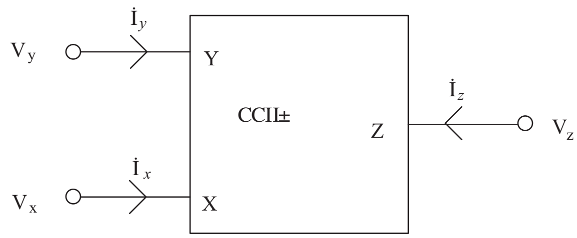


**Figure 5**. General structure of a CCII± device.

In the design, AD844 integrated circuit (IC) with current-feedback architecture is used as CCII+. The maximum output voltages of NHS state variables are about $\pm 40$ V. However, the maximum operating voltage of the AD844 IC is $\pm 18$ V. For this reason, state variables and initial conditions of the system are scaled by 15 as given in Eq. (8). The new names of state variables of the scaled NHS were given as $p, q, r, s$. Values of initial conditions of the NHS were taken as $p_0 = 0.0067$, $q_0 = 0.0067$, $r_0 = 0.0067$, $s_0 = 0.0067$.

$$\begin{bmatrix} i_y \\ V_x \\ i_z \end{bmatrix} = \begin{bmatrix} 0 & 0 & 0 \\ 1 & 0 & 0 \\ 0 & \pm 1 & 0 \end{bmatrix} \begin{bmatrix} V_y \\ i_x \\ V_z \end{bmatrix} \tag{7}$$

$$\begin{cases} p = \frac{x}{15} \Rightarrow \dot{p} = \frac{\dot{x}}{15}, \\ q = \frac{y}{15} \Rightarrow \dot{q} = \frac{\dot{y}}{15}, \\ r = \frac{z}{15} \Rightarrow \dot{r} = \frac{\dot{z}}{15}, \\ s = \frac{s}{15} \Rightarrow \dot{s} = \frac{\dot{s}}{15} \end{cases} \tag{8}$$

The equation for the scaled system is obtained as:

$$\begin{gathered} \dot{p} = a_1 p + a_2 q \\ \dot{q} = a_3 p + 15 a_4 q r sgn(15r) \\ \dot{r} = a_5 q + a_6 r + a_7 s \\ \dot{s} = a_8 r + a_9 s + a_{10} p \end{gathered} \tag{9}$$

The analog electronic schematic of the system (9) using CCII+s is given in Figure 6. The components used in the circuit consist of: twenty-two AD844 ICs, two AD633/ADmultiplier ICs, four condensers, and twenty-four resistors. The passive component values are as follows: $C_1 = C_2 = C_3 = C_4 = 400nF, R_1 = R_{13} = R_{15} = R_{18} = R_{23} = 2k\Omega$, $R_2 = 1.25k\Omega$, $R_3 = R_{16} = 1.6k\Omega$, $R_4 = R_7 = R_{14} = R_{19} = R_{24} = 1k\Omega$, $R_5 = 425\Omega$, $R_6 = 5k\Omega$, $R_8 = 19k\Omega$, $R_9 = 15k\Omega$, $R_{10} = 1.45k\Omega$, $R_{11} = 110\Omega$, $R_{12} = R_{20} = 1.82k\Omega$, $R_{17} = 370\Omega$, $R_{21} = 2.42k\Omega$, $R_{22} = 19.6k\Omega$. The system is powered by $\pm 15$ Vdc power supply.

The state variable $(p, q, r, s)$ values and the phase characterization of the analog electronic circuit design (Figure 6) are given in Figures 7 and 8, respectively. If Figures 2 and 8 are investigated together, it is seen that the circuit design outputs and numerical analysis results confirm each other. According to this result, the designed analog electronic circuit can be used in various engineering designs.

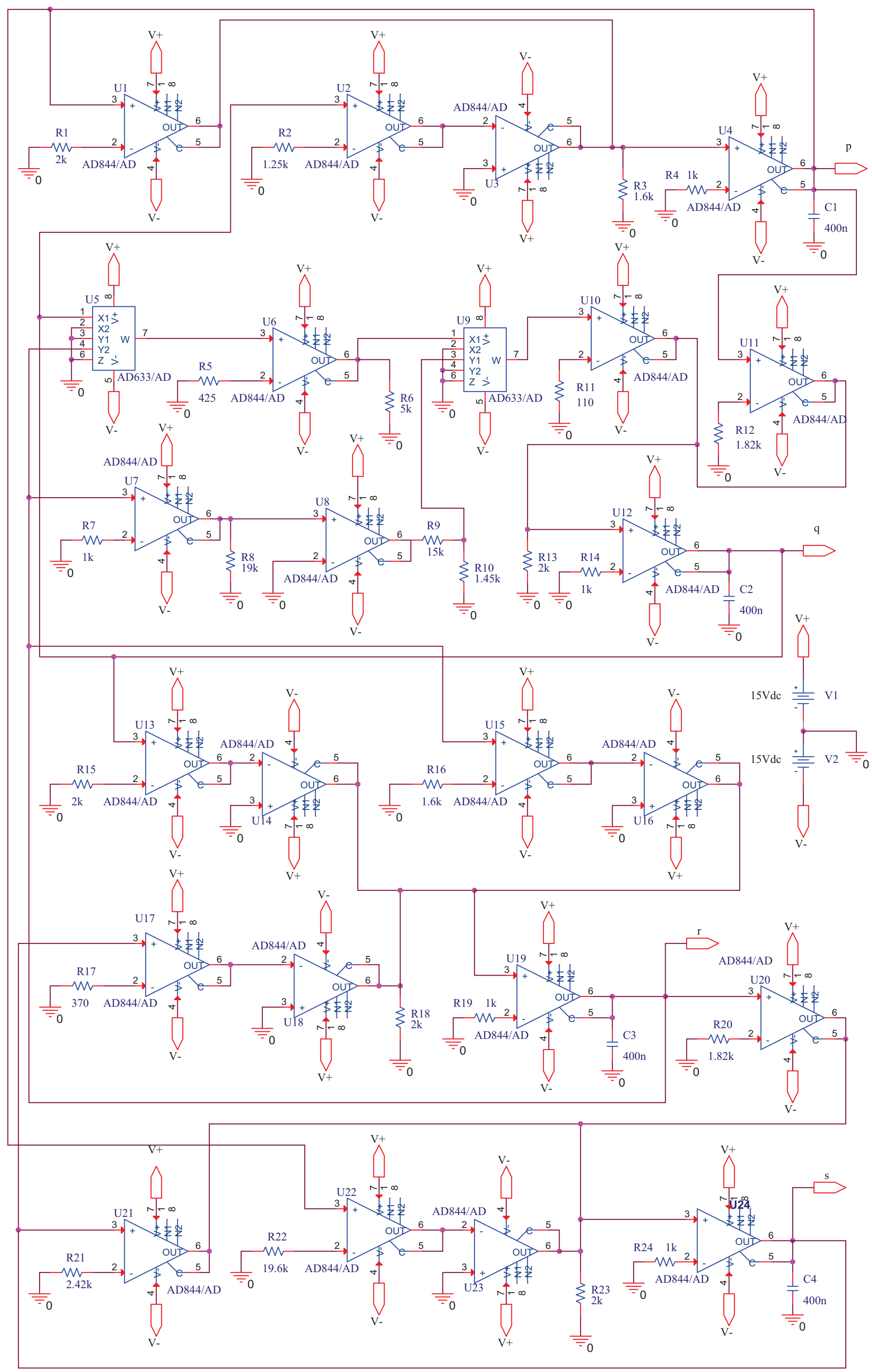


**Figure 6**. The electronic circuit design using CCII+s of the introduced NHS (9) for real engineering applications.

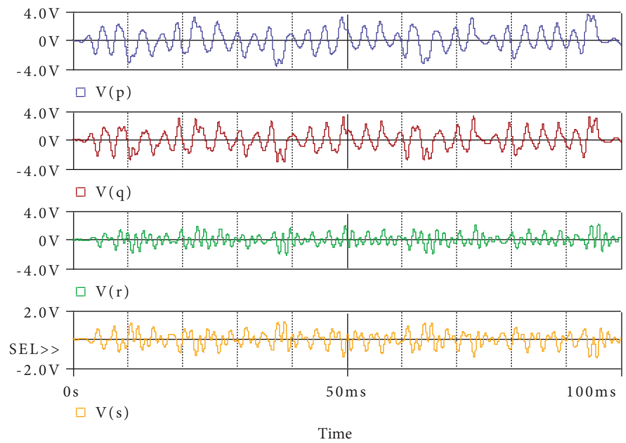


**Figure 7**. The outputs of the system (9) state variables $(p, q, r, s)$ of the analog electronic circuit design using CCII+s.

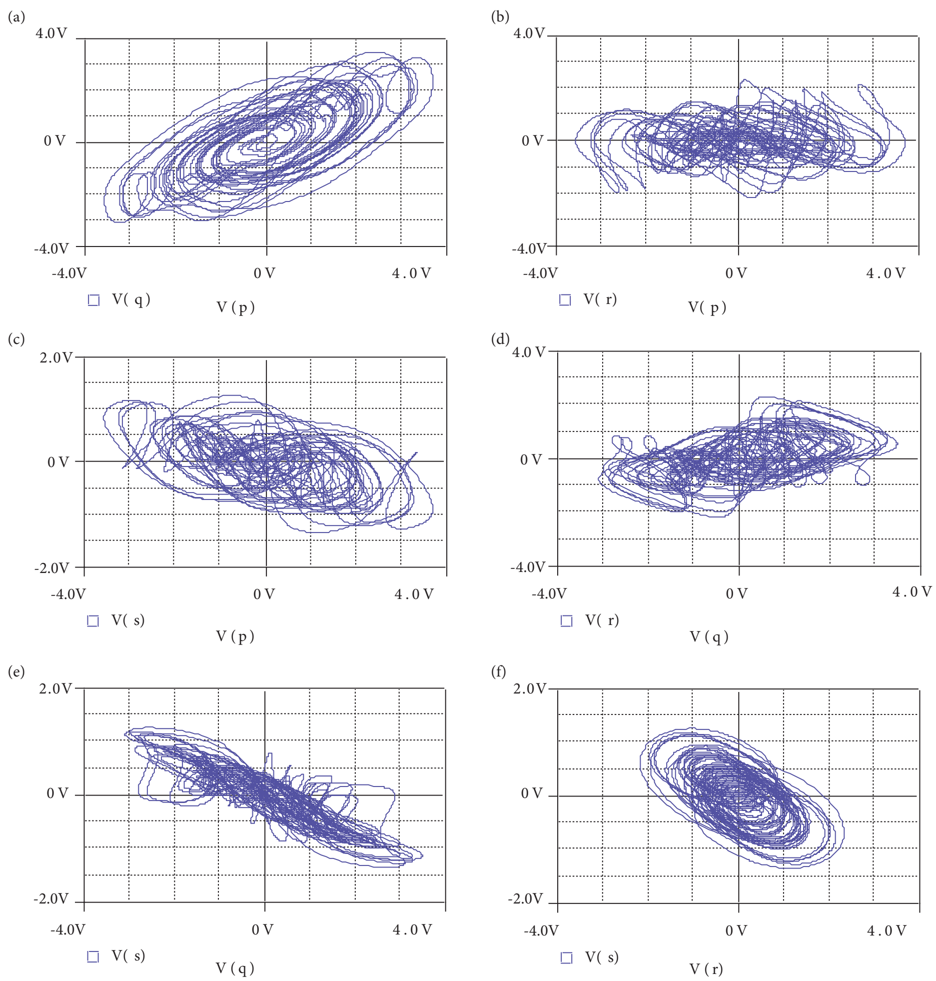


**Figure 8**. The phase characterization of the analog electronic circuit design using CCII+s of system (9) (a) for $p-q$ state variables, (b) for $p-r$ state variables, (c) for $p-s$ state variables, (d) for $q-r$ state variables, (e) for $q-s$ state variables, (f) for $r-s$ state variables.

## 4. Encryption application using the NHS

The introduced NHS can be used in applications such as chaos-based random number generator, chaos-based encryption, and chaos-based communication. In this context, an encryption design has been applied to demonstrate the use of the NHS in practical engineering applications. In the encryption application design, the output of state variable s is used as aperiodic information signal m to be encrypted. State variable r is used for encryption. The analog electronic circuit of the designed encryption application is given in Figure 9. Using the LM339 OPAMP ICs as a comparator, these two state variable outputs are converted to 1 (+ 5V) and 0 (0V) digital information. The information signal ($m$) and the chaotic signal ($r$) are processed XOR operation with each other to encrypt the information signal using by 7486 IC. An example of the information signal ($m$) with the encrypted signal ($e$) obtained from the circuit output is given in Figure 10.

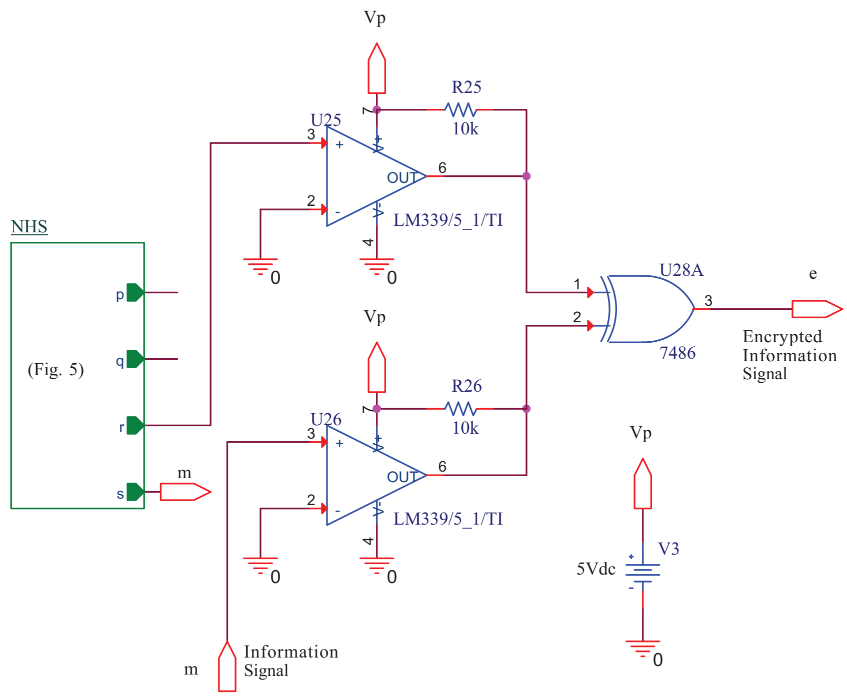


**Figure 9**. The analog electronic circuit of the designed encryption application using the introduced NHS.

The measure of the relationship between two variables can be determined by its covariance ($Cov$). For the relationship between two variables, the correlation coefficient ($\rho$) is used as a standard measure that is not affected by the change in measurement unit. The correlation coefficient is calculated as in Eq. (10) with the variance ($Var$) and the covariance of the two variables. The relation of two variables decreases as the correlation coefficient is closer to zero. The circuit in Figure 9 is run in Orcad-Pspice program and output values ($m$ and $e$) is saved in the file. The correlation coefficient between the information signal ($m$) and the encrypted signal ($e$) is $0.0078$. This shows that there is no significant relationship between the information signal and the encrypted signal.

$$\rho(x,y) = \frac{Cov(x,y)}{\sqrt{Var(x)Var(y)}} \tag{10}$$

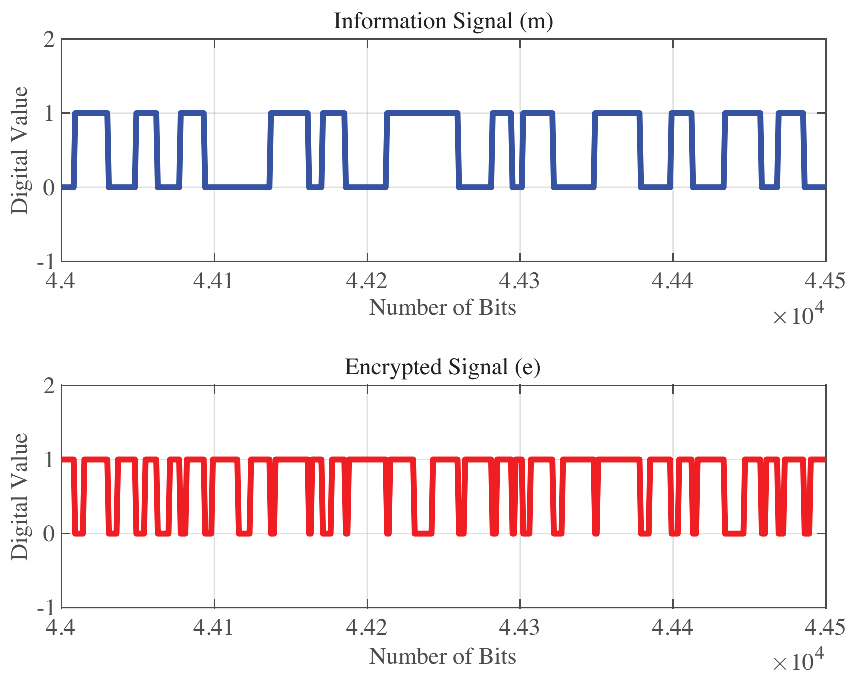


**Figure 10**. The sample of information and encrypted signals obtained from the circuit of designed encryption application in Figure 9.

## 5. Conclusion

In this study a novel HCS with a single nonlinear function is proposed. The simplicity in structure is highlighted and diverse dynamical behaviors such as the Eigen values, equilibrium points, stability, and LEs are analyzed. The hyperchaos is determined by finding two positive Lyapunov exponents. We used Wolf's algorithm to determine Lyapunov exponents. In order to show the complete dynamics of the system for parameter variation, we derived bifurcation diagrams and various limit cycle and attractor regions identified and discussed. We used forward–backward progression, and the multistable behavior of the system is identified and presented. We highlighted the advantages of the CCII+ method for the analog electronic circuit design and performed the same for the proposed HCS to show the easiness and effectiveness in real engineering applications. Moreover, an encryption design has been applied to demonstrate the use of the NHS in practical engineering applications. The correlation coefficient between the information signal and the encrypted signal is $0.0078$. As a result, the information signal has been successfully encrypted.

Similarly, random number generators (RNGs) application can be designed using the NHS. RNGs are important in cryptology, encryption, communication, and metaheuristic algorithm applications. Because chaotic signals are aperiodic, it can give good results to use in random number generation or encryption. However, using chaotic signals alone is not always successful in generating random numbers or encryption. Therefore, it may be necessary to use various preprocesses to increase the effect of chaotic signal. The preprocess method should be determined according to the characteristics of the used chaotic signal. Otherwise, using only chaotic signals without preprocess may not always give successful results.

## References

[1] Rossler OE. An equation for hyperchaos. Physics Letters A 1979; 71: 155-157. doi: 10.1016/0375-9601(79)90150-6

[2] Zhang B, Li H. A new four-dimensional autonomous hyperchaotic system and the synchronization of different chaotic systems by using fast terminal sliding mode control. Mathematical Problems in Engineering 2013. 2013: 179428. doi: 10.1155/2013/179428

[3] Khorashadizadeh S, Majdi MH. Synchronization of two different chaotic systems using Legendre polynomials with applications in secure communications. Frontiers of Information Technology & Electronic Engineering 2018; 19 (9): 1180-1190. doi: 10.1631/FITEE.1601814

[4] Mishkovski I, Kocarev L. Chaos-based public-key cryptography. In: Kocare L, Lian S (editors). Chaos-Based Cryptography: Theory, Algorithms and Applications. Heidelberg, Germany: Springer, 2011, pp. 27-30.

[5] Mèndez-Ramìrez R, Arellano-Delgado A, Cruz-Hernàndez C, Abundiz-Pèrez F, Martìnez-Clark R. Chaotic digital cryptosystem using serial peripheral interface protocol and its dsPIC implementation. Frontiers of Information Technology & Electronic Engineering 2018; 19 (2): 165-179. doi: 10.1631/FITEE.1601346

[6] Rostami MJ, Shahba A, Saryazdi S, Nezamabadi-pour H. A novel parallel image encryption with chaotic windows based on logistic map. Computers & Electrical Engineering 2017; 62: 384-400. doi: 10.1016/j.compeleceng.2017.04.004

[7] Kuiate GF, Rajagopal K, Kingni ST, Tamba VK, Jafari S. Autonomous Van der Pol-Duffing snap oscillator: analysis, synchronization and applications to real-time image encryption. International Journal of Dynamics and Control 2018; 19 (2): 1008-1022. doi: 10.1007/s40435-017-0373-z

[8] Rajagopal K, Laarem G, Vaidyanathan S, Karthikeyan A, Srinivasan AK. Dynamical analysis and FPGA implementation of a novel hyperchaotic system and its synchronization using adaptive sliding mode control and genetically optimized PID control. Mathematical Problems in Engineering 2017; 2017: 7307452. doi: 10.1155/2017/7307452

[9] Daltzis P, Vaidyanayhan S, Pham VT, Volos C, Nistazakis E et al. Hyperchaotic attractor in a novel hyperjerk system with two nonlinearities. Circuits, Systems and Signal Processing 2018; 37 (2): 613-635. doi: 10.1007/s00034-017-0581-y

[10] Hamdi B, Hassenr S. A new hypersensitive hyperchaotic system equilibria. International Journal of Bifurcation and Chaos 2017; 27 (5): 1750064. doi: 10.1142/S021812741750064X

[11] Hoang DV, Kingni ST, Pham VT. A no-equilibrium hyperchaotic system and its fractional-order form. Mathematical Problems in Engineering 2017; 2017: 3927184. doi: 10.1155/2017/3927184

[12] Rajagopa K, Karthikeyan A, Duraisamy P. Hyperchaotic Chameleon: fractional order FPGA implementation. Complexity 2017; 2017: 8979408. doi: 10.1155/2017/8979408

[13] Lassoued A, Boubaker O. Dynamic analysis and circuit design of a novel hyperchaotic system with fractional-order terms. Complexity 2017; 2017: 3273408. doi: 10.1155/2017/3273408

[14] Yang Q, Bai M. A new 5D hyperchaotic system based on modified generalized Lorenz system. Nonlinear Dynamics 2017; 88 (1): 189-221. doi: 10.1007/s11071-016-3238-7

[15] Luo X, Wang C, Wan Z. Grid multi-wing butterfly chaotic attractors generated from a new 3-D quadratic autonomous system. Nonlinear Analysis: Modelling and Control 2014; 19 (2): 272-285. doi: 10.15388/NA.2014.2.9

[16] Chithra A, Mohammed IR, Rizwana R. Observation of chaotic and strange nonchaotic attractors in a simple multi-scroll system. Journal of Computational Electronics 2018; 17 (1): 51-60. doi: 10.1007/s10825-017-1104-6

[17] Pehlivan İ, Uyaroğlu Y. A new chaotic attractor from general Lorenz system family and its electronic experimental implementation. Turkish Journal of Electrical Engineering & Computer Sciences 2010; 18 (2): 171-184. doi: 10.3906/elk-0906-67

[18] Çiçek S, Uyaroğlu Y, Pehlivan İ. Simulation and circuit implementation of Sprott case H chaotic system and its synchronization application for secure communication systems. Journal of Circuits, Systems and Computers 2013; 22 (4): 1350022. doi: 10.1142/S0218126613500229

[19] Xue W, Li Y, Cang S, Jia H, Wang Z. Chaotic behavior and circuit implementation of a fractional-order permanent magnet synchronous motor model. Journal of the Franklin Institute 2015; 352 (7): 2887-2898. doi: 10.1016/j.jfranklin.2015.05.025

[20] Chunbiao L, Pehlivan İ, Sprott JC. Amplitude-phase control of a novel chaotic attractor. Turkish Journal of Electrical Engineering & Computer Sciences 2016; 24 (1): 1-11. doi: 10.3906/elk-1301-55

[21] Zhang X, Li Z, Chang D. Dynamics, circuit implementation and synchronization of a new three-dimensional fractional-order chaotic system. AEU-International Journal of Electronics and Communications 2017; 82: 435-445. doi: 10.1016/j.aeue.2017.10.020

[22] Singh JP, Roy BK, Jafari S. New family of 4-D hyperchaotic and chaotic systems with quadric surfaces of equilibria. Chaos, Solitons & Fractals 2018; 106: 243-257. doi: 10.1016/j.chaos.2017.11.030

[23] Chithra A, Mohammed IR, Rizwana R. Observation of chaotic and strange nonchaotic attractors in a simple multi-scroll system. Journal of Computational Electronics 2018; 17 (1): 51-60. doi: 10.1007/s10825-017-1104-6

[24] Yu F, Li P, Gu K, Yin B. Research progress of multi-scroll chaotic oscillators based on current-mode devices. Optik 2016; 127 (13): 5786-5490. doi: 10.1016/j.ijleo.2016.03.048

[25] Trejo-Guerra R, Tlelo-Cuautle E, Carbajal-Gomez VH, Rodriguez-Gomez G. A survey on the integrated design of chaotic oscillators. Applied Mathematics and Computation 2013; 219 (10): 5113-5122. doi: 10.1016/j.amc.2012.11.021

[26] Peng Z, Wang C, Luo X. A novel multi-directional multi-scroll chaotic system and its CCII+ circuit implementation.Optik 2014; 125 (22): 6665-6671. doi: 10.1016/j.ijleo.2014.08.019

[27] Jothimurugan R, Suresh K, Ezhilarasu PM, Thamilmaran K. Improved realization of canonical Chua's circuit with synthetic inductor using current feedback operational amplifiers. AEU-International Journal of Electronics and Communications 2014; 68 (5): 413-421. doi: 10.1016/j.aeue.2013.11.004

[28] Lin Y, Wang C, He H. A simple multi-scroll chaotic oscillator employing CCIIs. Optik 2015; 126 (7-8): 824-827. doi: 10.1016/j.ijleo.2015.02.028

[29] Trejo-Guerra R, Tlelo-Cuautle E, Cruz-Hernandez C, Sanchez-Lopez C. Chaotic communication system using Chua's oscillators realized with CCII+s. International Journal of Bifurcation and Chaos 2009; 19 (12): 4217-4226. doi: 10.1142/S0218127409025304

[30] Sanchez-Lopez C. A 1.7 MHz Chua's circuit using VMs and CF+s. Revista Mexicana de Física 2012; 58 (1): 86-93.

[31] Ping Z, Li-Jia W, Xue-Feng C. A novel fractional-order hyperchaotic system and its synchronization. Chinese Physics B 2009; 18 (7): 2674. doi: 10.1088/1674-1056/18/7/009

[32] El-Sayed AMA, Nour HM, Elsaid A, Elsonbaty A. Dynamical behaviors of a new hyperchaotic system with one nonlinear term. Electronic Journal of Mathematical Analysis and Applications 2015; 3 (1): 1-18.

[33] Sprott JC. A Proposed standard for the publication of new chaotic systems. International Journal of Bifurcation and Chaos 2011; 21 (9): 2391-2394. doi: 10.1142/S021812741103009X

[34] Wolf A, Swift JB, Swinney HL, Vastano JA. Determining Lyapunov exponents from a time series. Physica D: Nonlinear Phenomena 1985; 16 (3): 285-317. doi: 10.1016/0167-2789(85)90011-9

[35] Schmitz R. Use of chaotic dynamical systems in cryptography. Journal of the Franklin Institute 2001; 338 (4): 429-441. doi: 10.1016/S0016-0032(00)00087-9

[36] Pisarchik AN, Jaimes-Reàtegui R, Sevilla-Escoboza JR, Ruiz-Oliveras FR, Garcìa-Lòpez JH. Two-channel optoelectronic chaotic communication system. Journal of the Franklin Institute 2012; 349 (10): 3194-3202. doi: 110.1016/j.jfranklin.2012.10.005

[37] Martìnez-Guerra R, Garcìa JJM, Prieto SMD. Secure communications via synchronization of Liouvillian chaotic systems. Journal of the Franklin Institute 2016; 353 (17): 4384-4399. doi: 10.1016/j.jfranklin.2016.08.011

[38] Sedra A, Smith KC. A second-generation current conveyor and its applications. IEEE Transactions on Circuit Theory 1970; 17 (1): 132-134. doi: 10.1109/TCT.1970.1083067

[39] Gupta A. A study on current conveyors and their applications. Journal of Multi Disciplinary Engineering Technologies 2015; 9: 10-17.

[40] Barboza R. Hyperchaos in a chua's circuit with two new added branches. International Journal of Bifurcation and Chaos 2008; 18 (4): 1151-1159. doi: 10.1142/S0218127408020884

[41] Wei Z, Moroz I, Sprott JC, Akgul A, Zhang W. Hidden hyperchaos and electronic circuit application in a 5D self-exciting homopolar disc dynamo. Chaos 2017; 27: 033101. doi: 10.1063/1.4977417

[42] Jia Q. Hyperchaos generated from the Lorenz chaotic system and its control. Physics Letters A 2007; 366 (3): 217-222. doi: 10.1016/j.physleta.2007.02.024

[43] Feng C, Cai L, Kang Q, Wang S, Zhang H. Novel hyperchaotic system and Its circuit implementation. Journal of Computational and Nonlinear Dynamics 2017; 10 (6): 0610121. doi: 10.1115/1.4029227

[44] Zheng S, Dong G, Bi Q. A new hyperchaotic system and its synchronization. Applied Mathematics and Computation 2010; 215 (9): 3192-3200. doi: 10.1016/j.amc.2009.09.060

[45] Wen-Bo L, Tang WKS, Guan-Rong C. Forming and implementing a hyperchaotic system with rich dynamics. Chinese Physics B 2011; 20 (9): 090510. doi: 10.1088/1674-1056/20/9/090510

[46] Yu S, Lü J, Chen G. A family of n-scroll hyperchaotic attractors and their realization. Physics Letters A 2007; 364 (3-4): 244–251. doi: 10.1016/j.physleta.2006.12.029

[47] Chen DY, Shi L, Chen HT, Ma XY. Analysis and control of a hyperchaotic system with only one nonlinear term. Nonlinear Dynamics 2012; 67: 1745-1752. doi: 10.1007/s11071-011-0102-7

[48] Zhou P, Ding R. A novel hyperchaotic system and its circuit implementation. Key Engineering Materials 2011; 467-469: 321-324. doi: 10.4028/www.scientific.net/KEM.467-469.321

[49] Yu F, Liu L, Shen H, Zhang Z, Huang Y et al. Dynamic analysis, circuit design, and synchronization of a novel 6D memristive four-wing hyperchaotic system with multiple coexisting attractors. Complexity 2020; 2020: 5904607. doi: 10.1155/2020/5904607

[50] Singh JP, Roy BK. Analysis of an one equilibrium novel hyperchaotic system and its circuit validation. International Journal of Control Theory and Applications 2015; 8 (3): 1015-1023.

[51] Yu F, Shen H, Liu L, Zhang Z, Huang Y et al. CCII and FPGA realization: a multistable modified fourth-order autonomous Chua's chaotic system with coexisting multiple attractors. Complexity 2020; 2020: 5212601. doi: 10.1155/2020/5212601